

FUEL ROD VIBRATIONS INDUCED BY COOLANT FLOW

A. FEDERICO, P. GRILLO,

Comitato Nazionale per l'Energia Nucleare, C.S.N.-Casaccia, Rome, Italy

ABSTRACT

A theoretical study of rod bundle vibrations induced by a coolant flow parallel to the rods is made as a support to mechanical design of fuel assemblies for light water reactors.

Mention is made to the experimental tests carried out on fuel assembly prototypes in isothermal and adiabatic conditions in order to compare predicted and measured data.

Discussion is also made about the application of this analysis to the design criteria for spacers of fuel bundle mechanically assembled.

INTRODUCTION

The CNEN is carrying out a complete program of design and evaluation of fuel for reloading in the light water cores, pressurized and boiling.

Between the problems created by the reload, partial or total, of a fuel assembly into an existing core, those ones related to the spacer grid constitutes, in any case, a critical point because they generally affect the entire design and the all performance parameters.

It has been already pointed out, as a design criteria, the fact of avoiding a monolithic configuration of fuel rods, assembling on the contrary those ones by finger types of spacers having with the rods spring or elastic contact.

With this solution, vibrations induced into the rods by coolant flowing parallel to their axis cause a sliding movement at the spacer contact points whose evaluation, in its type and extent, is of primary importance for the design choice of spacer performance parameters.

This paper deals with the activities carried out in order to investigate the fuel rod vibrations induced by coolant and their implication on fuel elements design for thermal reactors, that can be divided as follows:

- 1) Analytical approach to the phenomenon, with theoretical evaluation of the rods vibrational modes and of the corresponding displacements;
- 2) Experimental investigation on rods bundle, tested in condition very close to those of operation in the reactors;
- 3) Analytical methods performed for the vibrational data analysis and elaboration.

ANALYTICAL APPROACH

Since the rods, along their length, have some contact points with the spacers, they can be considered as beams of constant section and linear density constrained in N points.

Each rod is subjected to the forces exerted by the transversal turbulent component of the fluid flow, the elastic forces proportional to the rod bending stiffness, and the viscous friction actions of the coolant, to that for a portion of the rod between two constraints the general motion equation is:

$$EJ \frac{\partial^4 Y(x,t)}{\partial x^4} + m \frac{\partial^2 Y(x,t)}{\partial t^2} + d \frac{\partial Y(x,t)}{\partial t} = f(x,t)$$

where:

$Y(x, t)$ is the transversal displacement at time t of the point x of the rod;
 m is the mass of the rod per unit length;
 α is the viscous friction coefficient;
 EJ is the rod bending stiffness;
 $f(x, t)$ is the force acting on the rod due to the transversal turbulent component of the fluid flow.

This equation has been integrated on the basis of the following hypothesis:

- the action due to the turbulent component of the flow, $f(x, t)$ is considered to be represented at a generic point \bar{x} of the rod as the superposition of a certain number of forces, each of them having its own frequency and amplitude, i.e.,

$$f(\bar{x}, t) = \sum_K P_K(\bar{x}) \text{ sen } (\omega_K t + \varphi_K) \quad (2)$$

If we look then for a solution of the type:

$$Y(x, t) = \sum_n X_n(x) \cdot q_n(t) \quad (3)$$

which represents the rod motion by the superposition of an infinite number of allowed modes, each of which is a function of time multiplied by a function of the spatial coordinate, we obtain:

$$Y(x, t) = \sum_n X_n(x) \sum_K D_{nK} \text{ sen } (\omega_K t + \delta_{nK}) \quad (4)$$

where D_{nK} and δ_{nK} are suitably determined constants.

It is important to notice that eq. 2 is essentially the Fourier expansion of a periodic function, so that eq. 4 holds true for a periodic force of any kind.

Let us now consider the case in which the external force applied to the rod is represented by a number of shocks occurring randomly in time and space. In this case the damped natural vibrational modes of the rod will be excited, with boundary conditions given by the displacement and velocity of each point of the rod at the time of each shock. A shock like this could occur, if sudden fluctuations of flow or pressure would take place in the vessel where the rod is contained or if we consider the turbulent eddies acting randomly on the rod.

Because of the superposition principle we may state that if the external force is represented by a periodic force of the type described by eq. 2 with the addition of random shocks, the motion of the rod will be given by eq. 4 with the addition of the rod natural oscillations progressively

damped and then reexcited.

The frequency analysis of the motion of a point of the rod will therefore reveal the frequencies of the Fourier components of the periodic force acting on the point and the frequencies of the damped natural oscillations of the rod.

As the frequency analysis of the rods reported in this paper and in most others (1)(2)(3)(4) show that only the natural frequencies of the rods are excited, it is possible to conclude that the only steady periodic forces acting on the rods have frequency components very near to the rods natural frequencies.

This would be the case if a self sustained mechanism as suggested by Quinn (2) would be operative.

The other possibility is that the impact of turbulent fluid aggregates act as a random source of excitation of damped free vibrations and that no periodic force is actually present.

EXPERIMENTAL INVESTIGATION

Experiments were set up in support to the theoretical analysis in order to determine the frequency corresponding to the various vibrational modes of the individual pins and the amplitudes and phase of the initial vibrational modes together with the resulting strained position.

Measurements were made in a 16 and in a 36 rod bundles, under isothermal and adiabatic conditions, in single and two phase flow, at 30 and 70 ata.

As a sample, are reported in Figure 1 the mechanical characteristics of the 16-pin bundle and the coolant parameters investigated.

The instrumentation used, consisting of strain-gages and electromagnetic extensometers, was positioned as shown in Fig. 2: pins A, B and C are instrumented with "Microdot" strain-gages; pins E and D and the spacers and end plates are instrumented with differential shift transducers.

The measurement data were recorded on AMPEX magnetic tape and subsequently processed in an analog-digital computer.

Some initial tests were performed to determine the back-ground noise of the devices forming the measuring train and to assess the effect of the loop pump motion on the dynamic behavior in the test section.

Fig. 3 is a block diagram of the measuring system used, showing both the strain-gages and the differential shift transducers.

It should be noted that:

- the presence of oscillographs has made it possible to check each signal for the entire duration of the recording;
- the presence of the high-pass filters, used to eliminate the slow signal drifting, due to the instability of the electrical parameters of the measuring bridge resulting from the special environmental conditions under which the sensors had to operate.

The processing of data on the Hybrid computer ⁵ has furnished the power spectrum of each recorded signal, from the interpretation of which the desired information could be obtained.

Fig. 4 shows, by way of example, the power spectrum obtained from the signal of the differential transducer fitted on the second spacer.

An analysis of the power spectrum and of other data relating to single-phase fluid conditions shows that the frequency of the vibrational motion of the entire bundle is in the order of 15 ± 3 Hz. It is interesting to note that such frequency also corresponds to the basic vibrational mode of the entire bundle considered as a single girder.

A graph, versus the average fluid velocity, of the following quantity:

$$\mathcal{M} = \sqrt{\int_{12 \text{ Hz}}^{18 \text{ Hz}} F(f) df} \quad (5)$$

in which:

$F(f)$ represents the spectral function of the measuring unit μ^2/Hz , f is the frequency, yields the graph shown in Fig. 5, clearly showing the exponential-type dependence of the amplitude of shifts (in this case in RMS form) on the average fluid velocity.

Fig. 6 shows another type of power spectrum from a differential transducer fitted to a side pin.

Fig. 7 shows the data obtained from the analysis of the spectra from the three transducers fitted to the same side pin.

On the ordinates the parameter is the following quantity:

$$\mathcal{M} = \sqrt{\int_{52 \text{ Hz}}^{118 \text{ Hz}} F(f) df} \quad (6)$$

meaning that the integral was extended to the entire range of frequencies in which appear the power peaks relating to the basic vibrational modes of the individual pin.

As it can be seen, in all power spectra there is more than one peak

around the basic theoretical frequency of the pin, which can be explained by the following hypotheses:

- spatial asymmetry of the end and intermediate constraints (grids);
- position and number of the pin-spacer supporting points;
- influence of the contiguous pins, above all through the spacers;
- tolerances in the machining of the end plates-pin mating surfaces;
- possible pin detachments from one or more contact points with the spacers.

Fig. 8 shows the power spectrum from a strain-gage fitted to a central pin in the axial position shown, in which can be observed the power peaks in a 52 - 78 Hz range.

Fig. 9 shows other power spectra from strain-gages located midway on each span of the same central point.

The RMS value of the strains was calculated, as usual, in the 52 to 78 Hz frequency range, following the correlation:

$$\mu \varepsilon = \sqrt{\int_{52 \text{ Hz}}^{78 \text{ Hz}} P(f) df} \quad (7)$$

The data thus obtained from analog processing are now being theoretically analyzed to obtain the actual shift values relating to the strained configuration of the pins.

DATA ANALYSIS

Analysis of signals was made by digital methods on the basis of the fast Fourier transformation of sampled data series.

Fast Fourier transform subroutine works on data files ranging, in powers of 2, from 6 to 1024 data. There are two versions of FFT subroutine: the first one, of which is here shown some application example, performs real transformation on 1024 points in 1.2 seconds: the second one, that we use at present for cross spectral analysis, performs complex transformation on the same string of data in 1.2 seconds, at twice the speed of the first one.

Power spectral densities are computed through averaging of several Fourier transformations performed over successive strings of data. This method, that is known as the periodogram method, is not the best nor the faster one, but it is the only one possible with limited core memory computers. In Fig. 10 we can see as the method is applied on analog signals. Intervals between successive periodograms are employed to perform Fourier

transform, to square and to average squared values with those of the preceding section. Option is provided to perform computation with overlapping periodograms as it is shown in Fig. 10. In this case data acquisition is performed during operation of FFT, squaring and averaging subroutines, working in interrupt mode.

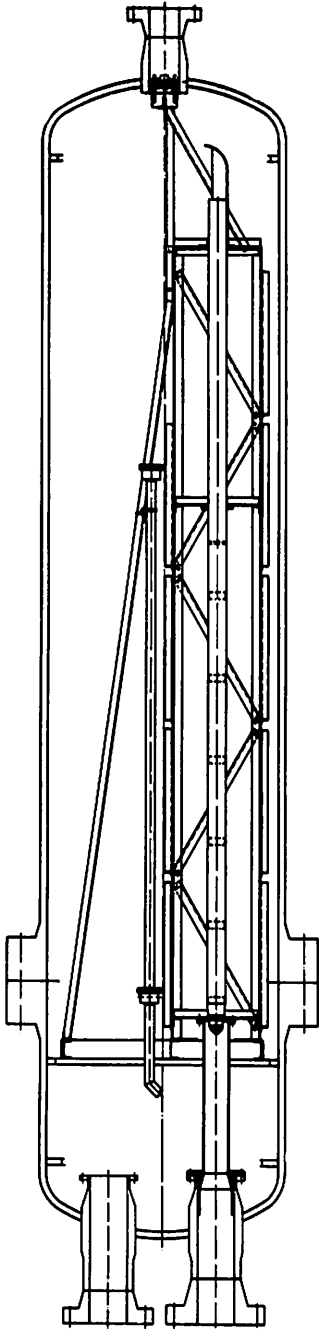
The programs operate in conversational way and under control of the operator: after each computation, the user can decide what will be next step and select it, using specified symbols on teletype, or digital switches.

For example, data output can be obtained on printer, plotter, or CRT, at request, depending on interest of the user in different forms of presentation. Integrated power spectral density is also computed and printed by means of that function; power indefinite frequency ranges can be easily evaluated.

General information about this program can be concluded with few considerations on computing time and economic charge per spectrum. Normally, if program operates on data recorded on magnetic tapes, we can adjust the playback speed to minimize sampling and computing time. Signals recorded at minimum speed can be played back 32 times faster. In the case of structural vibrations, computation is made in real time on frequency fields ranging from 1 to 400 - 500 Hz. Normal playback/record speed ratio is four: and computer works on signals whose maximum frequency is around 1,000 - 2,000 Hz. Sampling rate is at least twice the maximum frequency in the signal. In the standard case sampling time for a periodogram of 1024 data points is under 1 second: 1.5 second is employed in FFT, squaring and averaging operations. Power spectral density computation for 100 periodograms each of 1024 points, with a maximum frequency (in real time) of 2000 Hz, takes about 3 minutes. As mean value, with upper frequency of 1000 - 2000 Hz and 1024 points we spend 8 minutes per spectrum: on this basis it is possible to evaluate the cost of measurements on a medium size digital computer.

REFERENCES.

1. BURGREN ,BYRNES, BENFORADO , " Vibrations of Rods Induced by Water in Parallel Flow ", Trans. ASME 80 (1955) 991.
2. QUINN ."Vibration of Fuel Rods in Parallel Flow ", GEAP - 4059 (1962).
3. PAIDOUSSIN , " The Amplitude of Fluid Induced Vibration of Cilinders in Axial Flow" AECL -2225 (1965).
4. TIMOSHENKO - " Mechanical Vibration " - Van Nostrand (1957).



*ROD DIAMETER: 15 mm;
ROD LENGTH : 3000 mm;
SPACER : FINGER TYPE;
SPACER'S AXIAL POSITIONS:5;
COOLANT MASS VELOCITY: BETWEEN
 2×10^6 AND 10×10^6 kg/m²s;
COOLANT SUBCOOLING : BETWEEN
80°C AND 10°C;
COOLANT QUALITY: BETWEEN
2% AND 20%.*

FIG.1 - Vessel and test section

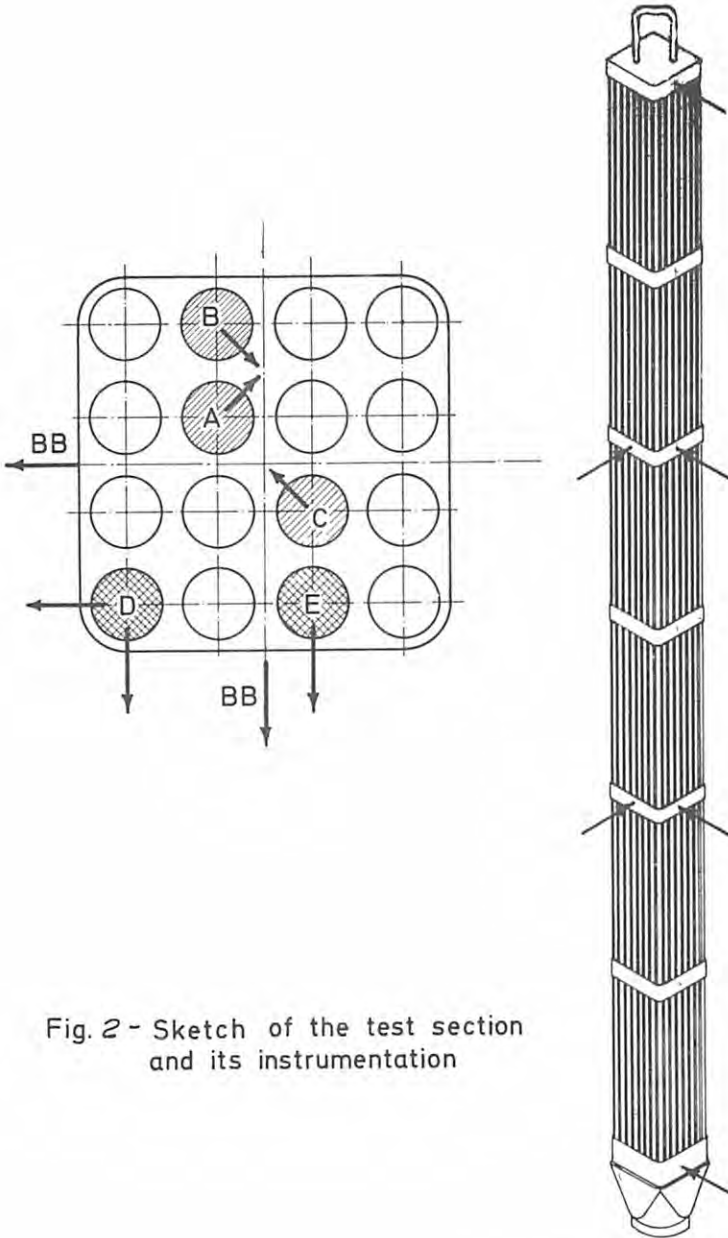


Fig. 2 - Sketch of the test section and its instrumentation

Sensor (BB) position for bundle vibrations.

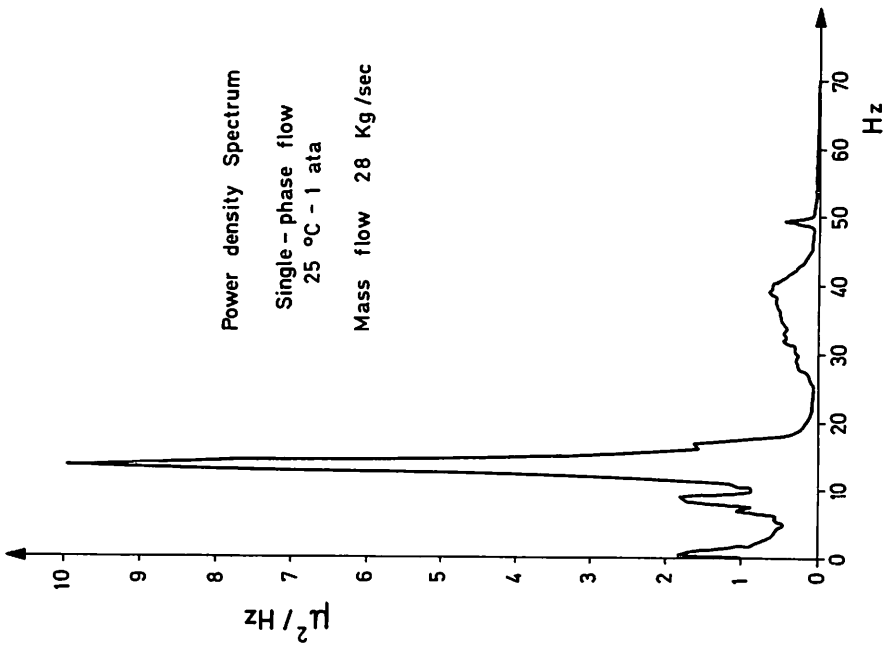


Fig. 4 - Power spectrum of the differential displacement transducer located at the second spacer.

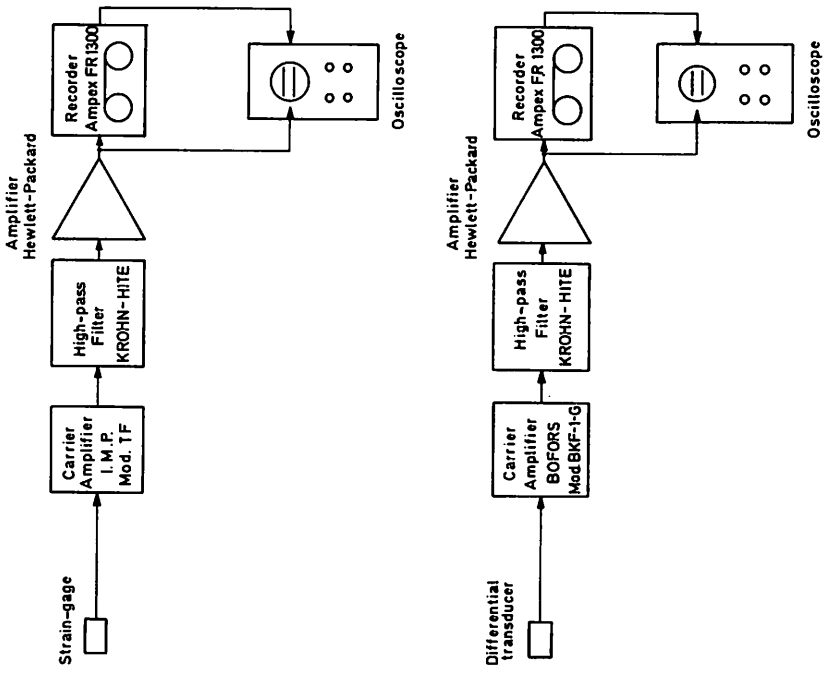


Fig. 3 - Block diagram of the measurement system.

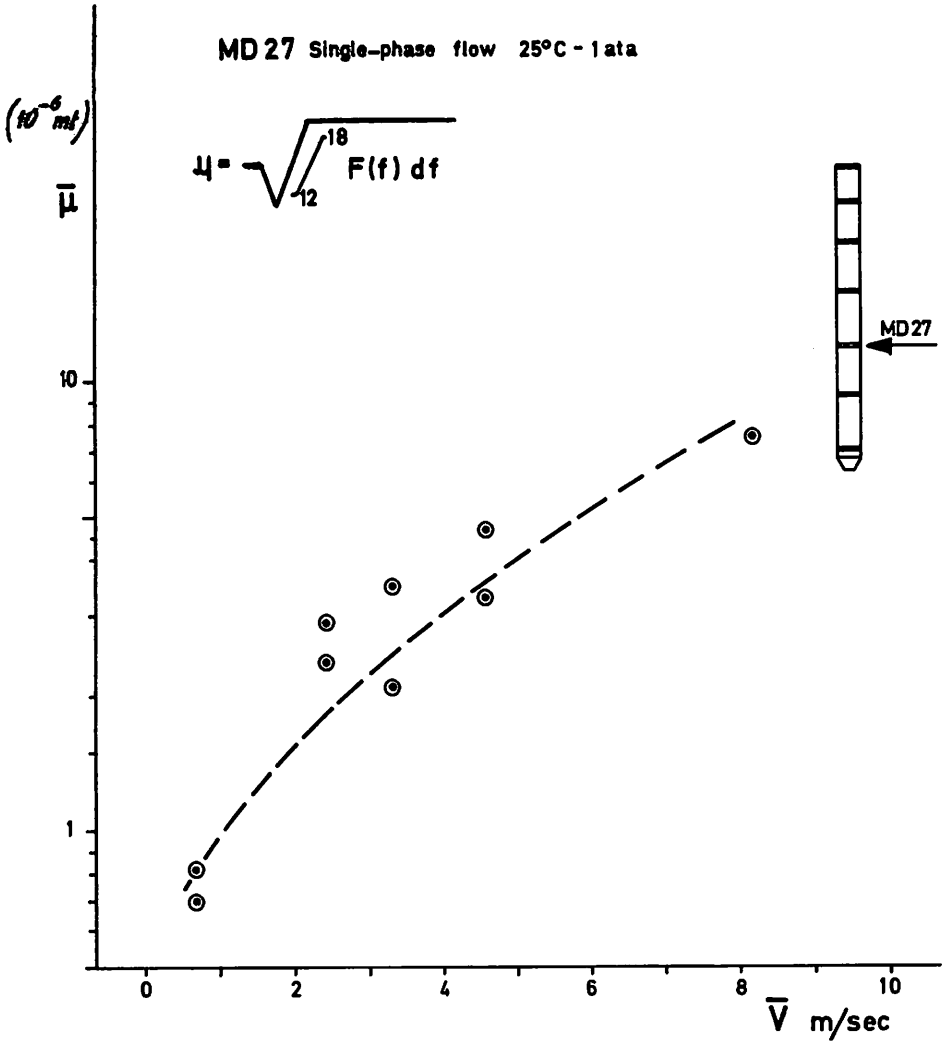


Fig. 5 - Displacement amplitude (as rms) versus linear fluid velocity.

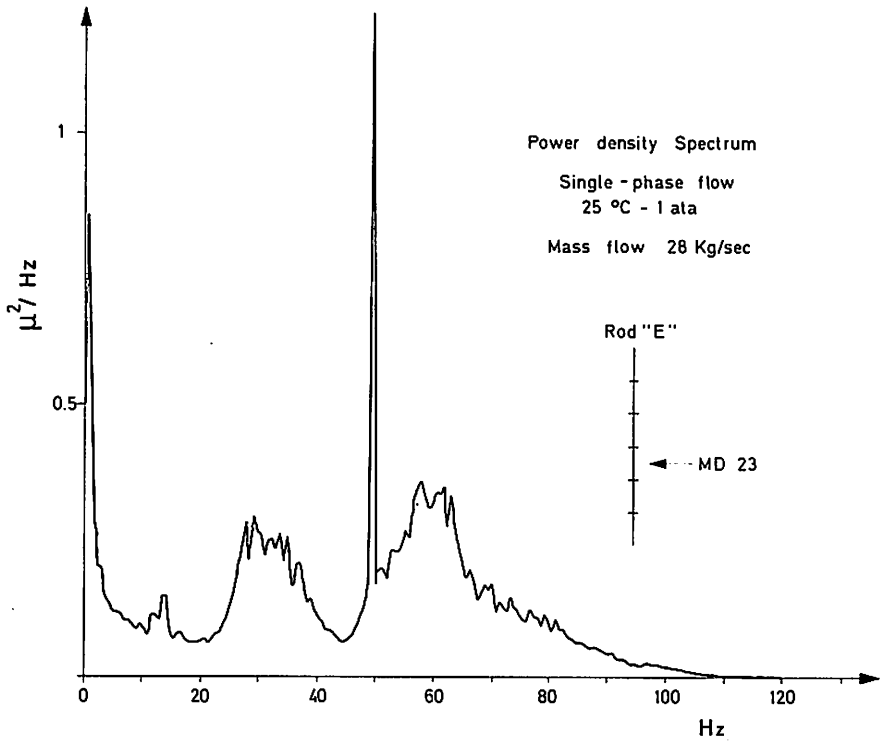


Fig. 6 - Power spectrum of the differential displacement transducer located at the side pin.

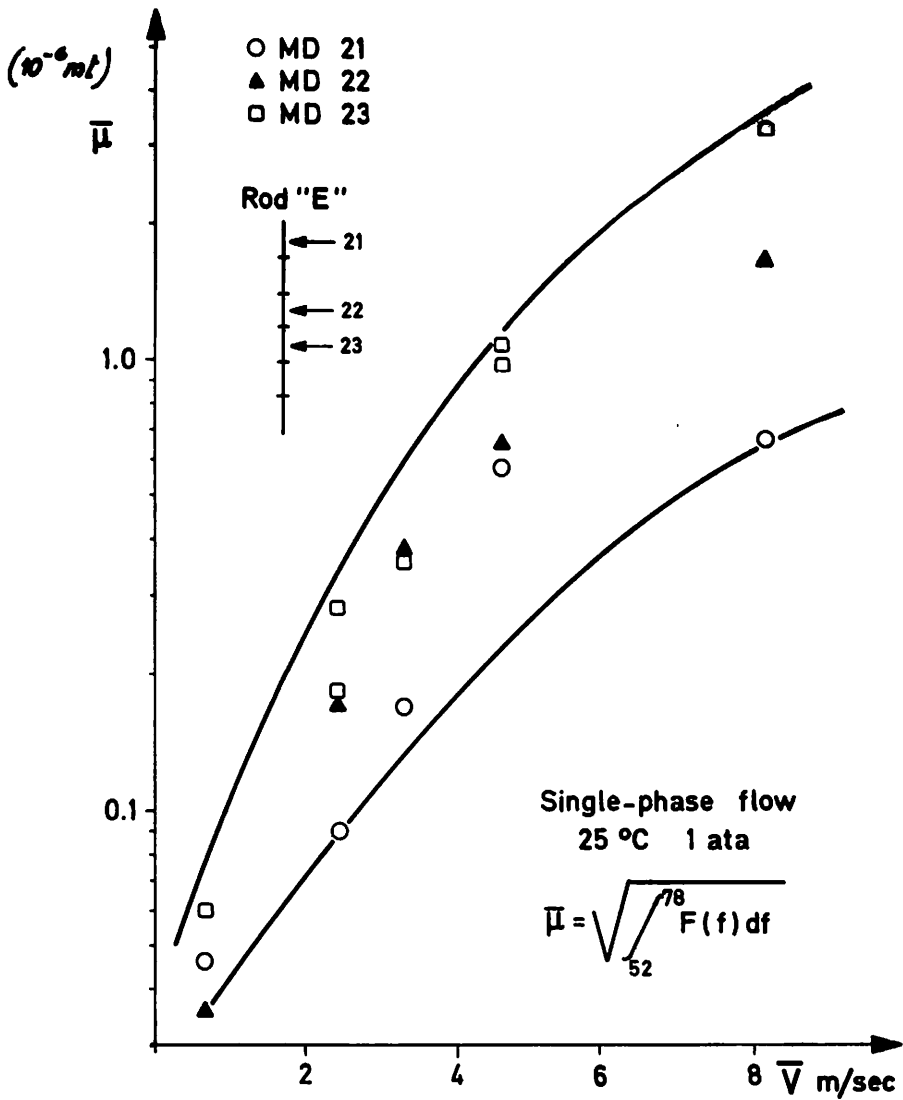


Fig. 7 - Displacement amplitude recorded at three axial points of the side pin, as a function of the average fluid velocity.

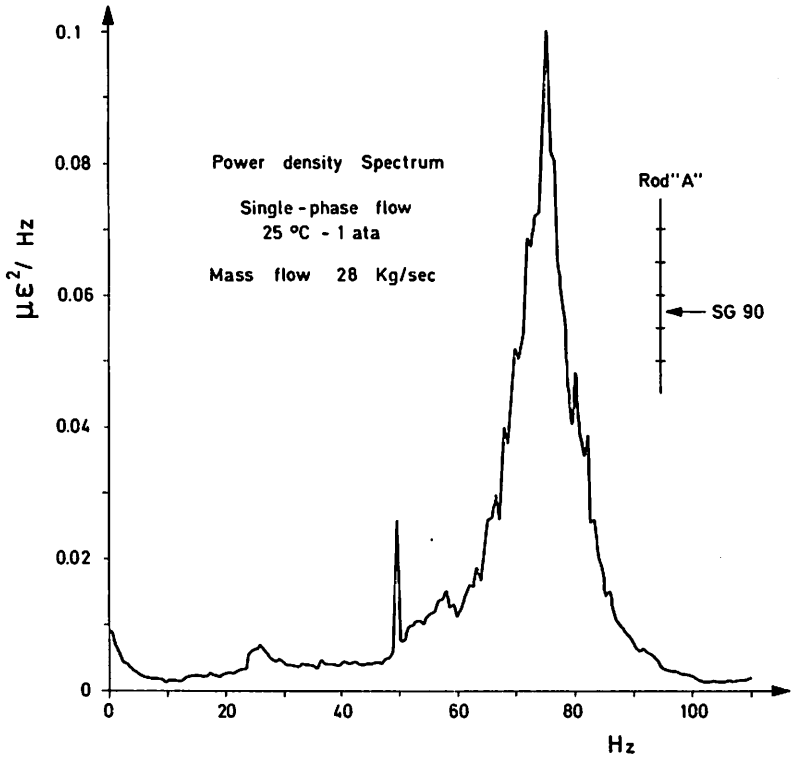


Fig. 8 - Power spectrum from the signal of the strain-gage, located in the central of the third span, for a central pin.

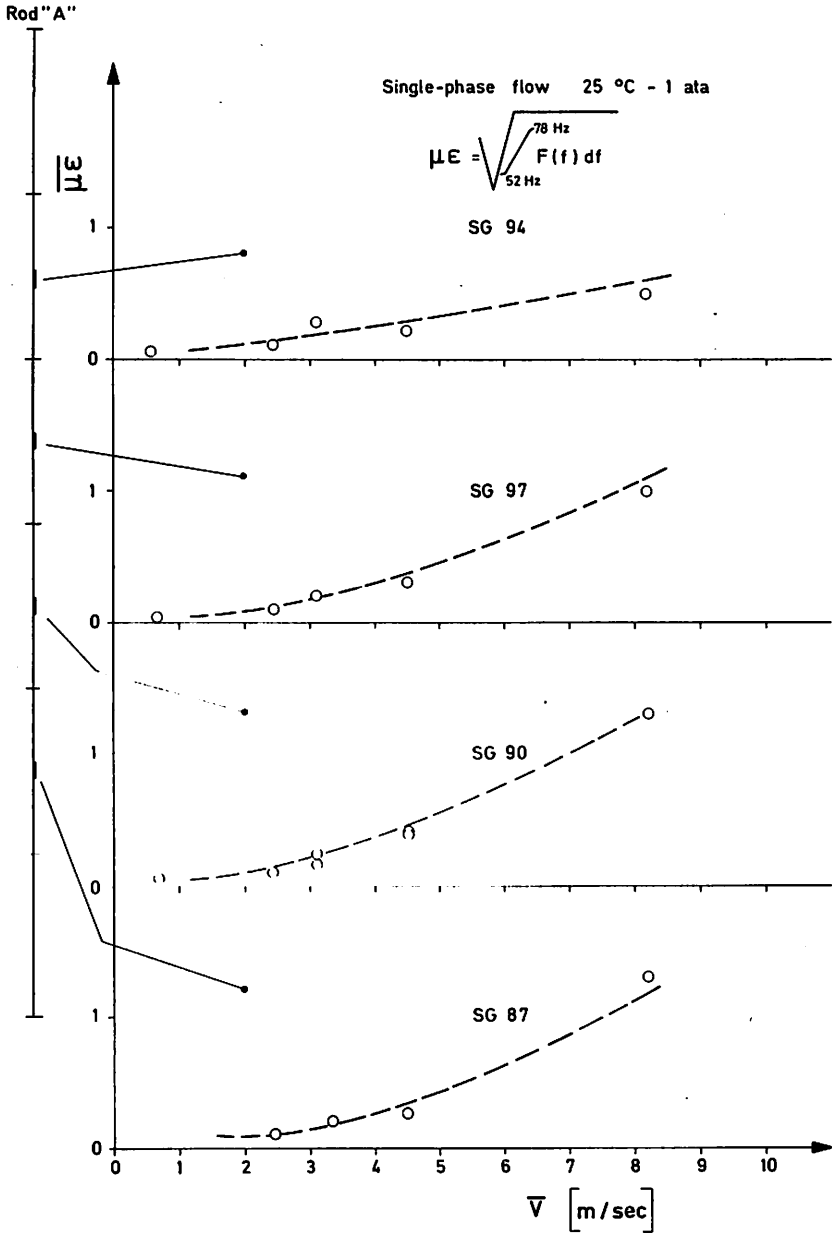


Fig. 9 - Strains detected from the strain-gages located in the central points of the spans of a central pin, versus the average fluid velocity.

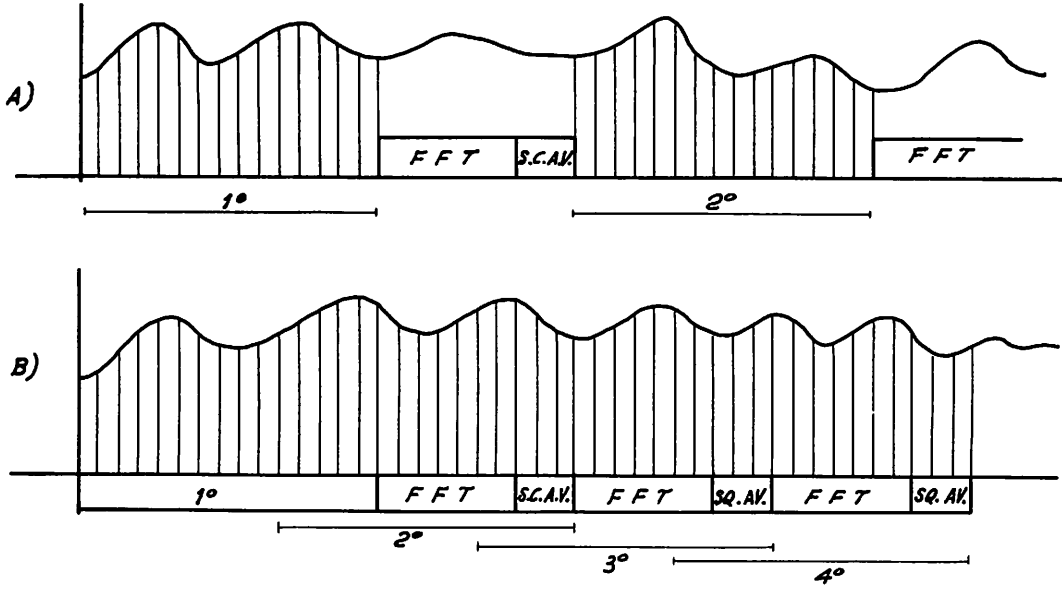


Fig.10 - Indications of the periodograms; A) Normal type; B) Overlapped type.

DISCUSSION

Q T. J. LEDWIDGE, Australia

What is the justification in limiting the measurement of the rms of the strain gauge reading to the energy between 52-78 Hz ? Is it true that the sharp resonance at 50 Hz was simply due to main frequency contamination ?

A P. GRILLO, Italy

The peak at 50 Hz is a consequence of a noise in the measurement chain and does not correspond to an actual vibration modus of the rod. Possible peaks at lower frequencies should correspond to the bundle vibration modii instead of pin vibration modii. So, as so far as single pin is concerned, the integral was limited to the mentioned frequency range of 52-78 Hz.

Q E. OHLMER, JRC Ispra, Italy

In your Fig. 21 you show the rms-values of the strains-gage-signals coming from different points of the tested rod. There are differences between these values. Are these differences in agreement with the modal deformation corresponding to the eigenfrequencies of the rod ?

A P. GRILLO, Italy

Strain-gages have been positioned in the span of the rod limited by two spacers, at the middle and at a quarter of the distance from spacers. First elaboration, not yet completed, shows that generally spacers act as a nodus and strained configuration of the rod shows two peaks between two subsequent spacers; but there are also more complicated strained configurations of the rod that are in an investigation phase.

Taking as reference a strained configuration with two peaks between spacers, it is possible to obtain indications for the different values shown in Fig. 21.

Q J. A. DEARIEN, U. S. A.

What are the dimensions on the ordinate of the graph in Fig. 19 ?

A P. GRILLO, Italy

Dimensions on the ordinate of the graph in Fig. 19 are micron (10^{-6} meter).